

A Cross-Power Spectral Density Method for Locating Oscillation Sources using Synchrophasor Measurements

Denis Osipov, *Member, IEEE*, Stavros Konstantinopoulos, *Member, IEEE*, Joe H. Chow, *Life Fellow, IEEE*

Abstract—This paper proposes a new measurement-based approach for locating the sources of forced or poorly damped oscillations in a power system. The approach is based on the concept of cross-correlation in the frequency domain known as cross-power spectral density (CPSD). CPSDs of synchronized voltage magnitude and voltage angle versus active power and reactive power signals obtained by phasor measurement units (PMUs) are computed using fast Fourier transform. The largest positive imaginary part of a CPSD is used as an indicator of the oscillation source. The type of an oscillation source is determined by comparing the spectral densities of active and reactive power. In addition, preprocessing of the signals is performed via variational mode decomposition for extracting the dynamic component of the signals. The proposed approach was able to successfully identify all submitted test cases in the IEEE-NASPI Oscillation Source Location Contest. Several case studies presented in this paper highlight the advantages of the proposed approach compared to the state-of-the-art dissipating energy flow method.

Index Terms— Forced oscillations, cross-correlation, cross-power spectral density, phasor measurement units, variational mode decomposition.

I. INTRODUCTION

PHASOR measurement units (PMUs) [1] find widespread use in power grids in the United States and around the world. These devices report voltage and current measurements, which are synchronized using the GPS signal, at 30 (25) or 60 (50) times per second for systems with nominal frequency of 60 (50) Hz.

The fast-reporting rate and data synchronization make PMUs a valuable tool for power system operators, which can record and analyze system events including oscillations. Oscillations observed in real power system operation can be either forced or due to poorly damped natural modes of the system. Identification of the causes of the oscillations requires locating the source, which is a challenging task. The additional challenge of identification is that the cause of the oscillations in power systems can be a malfunction due to improper tuning or operation of the power plant equipment such as governors, exciters, and power system stabilizers (PSS), HVDC systems, and converters used in interfacing renewable resources to the AC power grid. Most of such malfunctioning are not represented in the system models. Moreover, if the condition of

sustained oscillations in the system is not addressed, it can lead to equipment damage or in the worst-case scenario, blackout of a certain area in the system. Thus, a robust method to accurately identify the source(s) of the oscillations is important for power system operation. The method should also be applicable to PMU data away from the oscillation source, allowing the orientation and the nature of the sources to be identified.

Currently the dissipating energy flow (DEF) method [2] seems to be the most effective method for locating the source of the oscillations and has been successfully used by system operators. The DEF method, which was introduced in [3] and improved in [4] by adding signal band-pass filtering, calculates incremental energy [5] based on the energy function described in [6], [7]. References [8], [9] show that DEF may not correctly identify the source of oscillation under some load characteristics and for oscillations caused by excitation systems. Another limitation of DEF is its inability to determine whether the oscillation is caused by the excitation system (primarily reactive power control) or by the governor (primarily active power control). Thus, it is desirable to develop a method with improved oscillation source location identification and ability to discriminate the active or reactive power nature of the oscillation source.

In this paper we propose a new approach for locating the source of oscillations based on the cross-correlation of the measured signals. The concept of cross-correlation was successfully used in [10] to detect the presence of the oscillations. Reference [11] used the cross-spectral density, which is the cross-correlation in the frequency domain, to estimate mode shapes, while [12] used the cross-spectral density to track damping contribution of generators in the system. In the proposed approach three cross-correlations of measured signal deviations: voltage angle versus active power, voltage magnitude versus active power, and voltage magnitude versus reactive power, are separately analyzed in the frequency domain in the form of cross-power spectral densities (CPSD) to locate the source of the oscillation. In addition, power spectral densities (PSD) of active and reactive power are compared to determine the type of malfunctioning controllers that causes the oscillation. To effectively utilize the measured quantities and improve the accuracy of the source identification, it is necessary to perform preprocessing of the data by removing the quasi-

This work was supported in part by the Engineering Research Center Program of the NSF and the DOE under the supplement to NSF Award Number EEC-1041877, the CURENT Industry Partnership Program.

D. Osipov and J. H. Chow are with the Department of Electrical, Computer, and Systems Engineering, Rensselaer Polytechnic Institute, Troy, NY 12180 USA (e-mail: osipod@rpi.edu; konsts@rpi.edu; chowj@rpi.edu).

S. Konstantinopoulos was with the Department of Electrical, Computer, and Systems Engineering, Rensselaer Polytechnic Institute, Troy, NY 12180 USA. He is now with the Grid Operations and Planning group, Electric Power Research Institute, Palo Alto, CA 94304 USA (e-mail: skonstantinopoulos@epri.com)

steady state component of the signal using variational mode decomposition (VMD) [13]. It is assumed that the presence of the oscillation is already detected using one of the methods described in [14]-[15].

The proposed approach won first place in the IEEE-NASPI Oscillation Source Location (OSL) Contest [16]. The following are the features of the proposed approach: 1) requires only measurements of voltage and current phasors and some topological information if the source of the oscillation is not measured; 2) performs well when active power consumed by loads depends on voltage magnitude (voltage-sensitive loads); 3) identifies the type of the oscillation source (excitation systems, governors, etc.); 4) does not require band-pass filtering of measured signals. The aforementioned features are attributed to the three major contributions of the approach: 1) the additional CPSD describing cross-correlation between voltage magnitude and active power that ensures the correct identification of the oscillation source when the load active power depends on voltage magnitude; 2) comparison of PSDs of active and reactive power to correctly identify the type of the oscillation source; 3) VMD-based dynamic component extraction.

The rest of the paper is organized as follows. Section II describes the proposed approach, including the concepts of cross-correlation, cross-power spectral density and variational mode decomposition. In Section III case studies using simulated data from the 179-bus and 240-bus Western Electricity Coordinating Council (WECC) systems as well as actual PMU measurements are carried out to validate the proposed approach and compare it with the dissipating energy flow method.

II. DESCRIPTION OF THE PROPOSED APPROACH

In this section the main concepts of the developed approach are presented in details. The oscillation source problem is illustrated in Fig. 1, showing potential sources of oscillations such as generators, HVDC systems, wind turbines, and active loads. To identify the oscillation sources, PMUs are installed in the system to monitor the bus voltage phasors, and the active and reactive power flows (calculated from the current phasors) on the transmission lines.

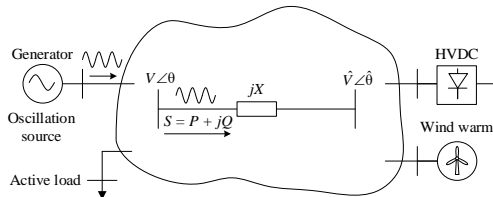


Fig. 1. Power and voltage oscillation measurements on a branch of the system.

A. Cross-correlation

Given a lossless branch with reactance X and under the assumption of $\sin(\theta) \approx \theta$ and $\cos(\theta) \approx 1$ for small values of θ the active power P and reactive power Q at the sending end of the branch can be calculated as

$$P = \frac{1}{X} V \hat{V} (\theta - \hat{\theta}), \quad Q = \frac{1}{X} V (V - \hat{V}) \quad (1)$$

where V and \hat{V} are, respectively, the voltage magnitudes at the sending end and the receiving end of the branch, and θ and $\hat{\theta}$ are, respectively, the voltage angles at the sending end and the receiving end of the branch, as shown in Fig. 1.

If V and θ are considered to be the inputs, and P and Q are considered the outputs, the input-output relationship can indicate the source of the oscillation. Specifically, if any output signal is leading the input signal as shown in Fig. 2, the source of a forced or poorly damped oscillation is located at the sending end of the branch or in the region connected to the sending end of the branch.

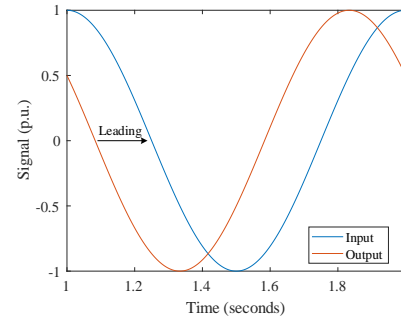


Fig. 2. Forced oscillation example of an output signal leading an input signal.

This oscillation source notion can be further illustrated by considering the sending bus as the terminal bus of a generator. The oscillation seen in the terminal voltages will be reacted to by the control equipment. The time constants in the control action will be manifested as delays in the P and Q outputs of the generator. Conversely, if the malfunctioning generator is the source of the oscillation, its P and Q outputs will lead the voltage oscillation, which is the result of how the power system as a whole is accommodating the oscillation source.

This input-output relationship can be formulated mathematically as a cross-correlation between an input and an output. Cross-correlation calculation is advantageous in the frequency domain as it can be readily computed using Fourier transform and no filtering of the signals is required. In the frequency domain the input-output cross-correlation becomes the input-output CPSD that is computed by multiplying element-wise, that is, the respective frequency points, the conjugate of the input PSD by the output PSD. From (1), three input-output CPSDs can be computed as

$$S_{\theta P} = \overline{\mathcal{F}\{\theta\}} \circ \mathcal{F}\{P\}, \quad S_{VP} = \overline{\mathcal{F}\{V\}} \circ \mathcal{F}\{P\}, \quad S_{VQ} = \overline{\mathcal{F}\{V\}} \circ \mathcal{F}\{Q\} \quad (2)$$

where $\mathcal{F}\{\}$ is Fourier transform, \circ denotes the Hadamard product, which is the element-wise product, and $\overline{}$ denotes the conjugate. Note that the correlation between θ and Q is generally small and does not provide additional information in terms of locating the source of the oscillation compared to other three cross-correlations. In terms of the limitations of CPSD a long window of data is required for good frequency resolution for signals with low amplitude and frequency of the oscillation. In order to obtain higher frequency resolution, the use of windowing utilized by methods such as short-time Fourier transform or Stockwell-transform is avoided.

The case of an output signal leading an input signal corresponds to a positive imaginary part of the input-output CPSD or to an input-output CPSD angle in the range from 0° to 180° as shown in Fig. 3. The source of the forced oscillation can be identified by looking at the branch with the largest imaginary part of CPSD. If this branch is a radial branch connected to a generator, load or HVDC terminal, the source is identified. If the branch is a part of ring or meshed topologies, multiple CPSD flows need to be analyzed.

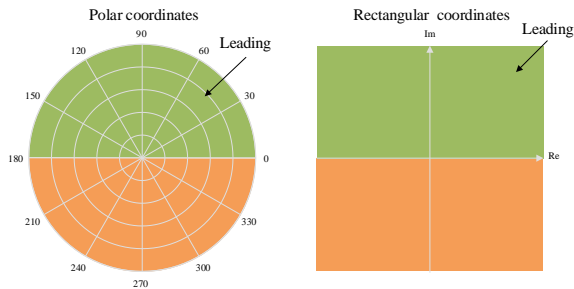


Fig. 3. CPSD areas in polar and rectangular coordinates when an output signal leads an input signal.

B. CPSD flow

The Appendix shows that CPSD is related to dissipating energy, that is, $S_{\theta P}$ and S_{VQ} correspond to the first and second components of the dissipating energy, respectively. Hence, according to the DEF method [4], the CPSD flows satisfy Kirchhoff's current law. Another justification for CPSD flows to satisfy Kirchhoff's current law is the fact that for a set of branches connected to the same bus the sum of active and reactive power signals will be equal to zero, while the voltage magnitude and voltage angle signals of all branches will be almost identical (actual voltage measurements can be slightly different due to accuracy of potential transformers and non-zero resistance of busbars at a substation). Using this fact and the topological information of the system, further analysis of CPSDs to locate the oscillation in the ring or meshed topologies can be performed. For each bus a combined CPSD inflow and outflow through the branches that are connected to the bus is calculated by adding the imaginary parts of CPSDs of the branches with negative and positive values, respectively. In addition, if the measurements to define the source of oscillations are provided for only one of multiple parallel branches, the other branches are assumed to carry the same flow. Even though this assumption is not true for all parallel branches in a real system, in most cases the difference between the parameters of the parallel branches is sufficiently small. If the outflow from the bus is substantially larger than the inflow, the controlled equipment on the bus is the source of the oscillation; otherwise, this bus is classified as an intermediary bus. However, if a bus with the largest outflow is on the opposite end of the branch (which does not have PMU measurements), it can indicate that either this bus is the source or that the source is located in the region connected to this bus.

C. Type of the Source Identification

To identify the type of the oscillation source, we propose an intuitive approach based on the fact that malfunction of active

power control equipment will manifest itself more in oscillations of active power, while reactive power control equipment will manifest itself more in oscillations of reactive power. Therefore, to formalize such dependencies in the frequency domain, PDS of active power ($S_P = \mathcal{F}\{P\}$) and reactive power ($S_Q = \mathcal{F}\{Q\}$) from all measured branches in the system are analyzed. If $\max(|S_P|) > \max(|S_Q|)$ then the source is P-type, i.e., a generator governor (controlling active power output of a generator), a cyclic load including induction motors (defined by periodic change in active power consumption) or the sending end of an HVDC system (controlling active power transmitted from the AC network). However, if $\max(|S_P|) < \max(|S_Q|)$ then the source is Q-type, i.e., an excitation system (controlling the voltage magnitude by changing the reactive power output) or the receiving end of an HVDC system (maintaining the set-point for voltage magnitude at the inverter terminal). For a P-type source the oscillation is observed in the active power signal; however, for a Q-type source of oscillation is observed in both the active and reactive power signals. Thus, if $\max(|S_P|) \cong \max(|S_Q|)$ then the source is assumed to be Q-type.

The maximum absolute values of the signal PSDs of all measured branches, not only the branch of the likely source of the oscillation determined by analysis of CPSDs, are compared with each other based on the understanding that active and reactive power controls are decoupled to a certain degree. Moreover, if there is a malfunction in an excitation system, it will cause oscillations in reactive power not only at the source of the oscillation, but also in other locations. Specifically, the malfunction will trigger a response of reactive power controls of other generators in the system which will also manifest in reactive power oscillations coming from these generators. A similar relationship is true for the case of a governor and active power.

D. Dynamic component extraction

In contrast to simulated data the actual signals measured by PMUs in power systems consist of not only a dynamic component which represents the oscillations but also of the quasi-steady state component [17] which represents variation of measured quantities in response to continuously changing loading conditions and noise, as the oscillations tend to persist for tens of seconds and minutes. The quasi-steady state component and noise can be removed in the signal analysis of (2). As a result, extracting only the dynamic component from the data can improve the accuracy of oscillation source identification.

In this work we propose to use the variational mode decomposition (VMD) [13] to extract the dynamic components of the signal. In essence VMD decomposes a signal into a set of N components which are called intrinsic mode functions (IMFs). If the IMFs are arranged from the fastest varying to the slowest varying, the last IMF corresponds to quasi-steady state component of the signal, while the residual of the

decomposition corresponds to the noise. As a result, the dynamic components can be obtained by combining IMFs from the first to the $(N-1)$ th components. In Fig. 4 an actual signal measured by PMU and the quasi-steady state component obtained by VMD are shown. The signal in Fig. 4b obtained from the original signal in Fig. 4a contains only aperiodic variations and an increasing trend that capture the change in loading conditions, but it does not have any dynamics. Subtracting this quasi-steady state component from the original signal would result in a multi-frequency signal with an average value of zero, as shown in Fig. 5. In addition to the variation mode decomposition, we have evaluated the following methods: intrinsic time-scale decomposition, maximal overlap discrete wavelet transform, and empirical mode decomposition. Fig. 6 shows the comparison of four evaluated methods with respect to quasi-steady state component estimation. The VMD provides better performance in terms of quasi-steady state component estimation by capturing not only the increasing trend, but also the aperiodic variations of active power. This allows VMD to perform better dynamic component extraction.

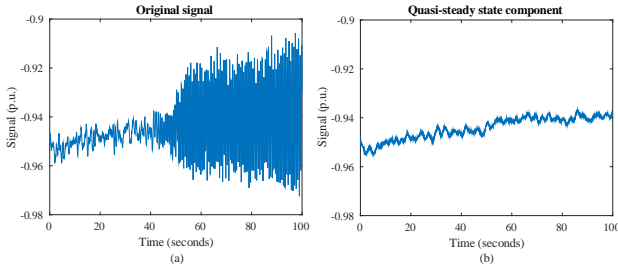


Fig. 4. Example of quasi-steady state component (b) obtained from a measured signal (a).

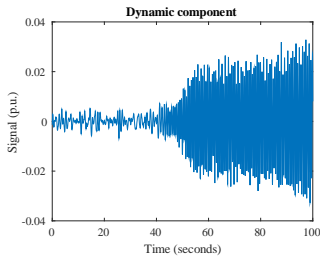


Fig. 5 Example of dynamic components obtained from a measured signal.

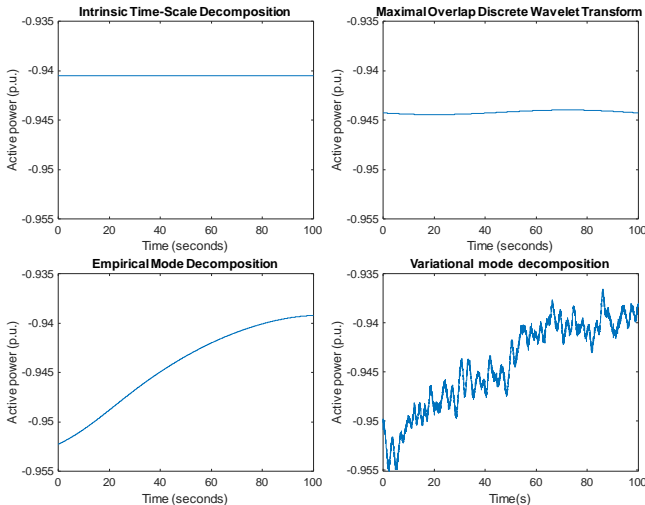


Fig. 6 Comparison of quasi-steady state components obtained using four different methods.

E. Oscillation source identification algorithm

The concepts described in Sections II.A – II.D are combined to establish the following identification algorithm.

1. Group together current phasors and voltage phasors measured at the sending end of a branch and calculate the active and reactive power flows.
2. Perform VMD on the voltage magnitudes, voltage angles, active powers, and reactive powers to obtain intrinsic mode functions (IMFs). The last IMF represents the quasi-steady state component.
3. Reconstruct the dynamic components by adding IMFs from the first to the penultimate IMF. This operation leaves only the dynamic components ΔV , $\Delta \theta$, ΔP , and ΔQ .
4. Perform fast Fourier transform (FFT) to calculate PSDs S_P and S_Q , using ΔP and ΔQ .
5. Find the index i that corresponds to the largest absolute value of PSDs. This index corresponds to the frequency of the oscillation to be investigated.
6. Identify the type of the source. If $\max(|S_{P_i}|) > \max(|S_{Q_i}|)$ then the source is a P-type. If $\max(|S_{P_i}|) < \max(|S_{Q_i}|)$ or $\max(|S_{P_i}|) \approx \max(|S_{Q_i}|)$, then the source is a Q-type.
7. Perform FFT to calculate the three CPSD quantities $S_{\theta P}$, S_{VP} , and S_{VQ} in (2) using ΔV , $\Delta \theta$, ΔP , and ΔQ from Step 3.
8. If $\max(\text{Im}(S_{\theta P_i})) \gg \max(\text{Im}(S_{VQ_i}))$ and $\max(\text{Im}(S_{\theta P_i})) \gg \max(\text{Im}(S_{VP_i}))$ use $S_{\theta P_i}$ to find the largest positive imaginary part. If $\max(\text{Im}(S_{VP_i})) > \max(\text{Im}(S_{VQ_i}))$, use S_{VP_i} to find the largest positive imaginary part. Otherwise, use S_{VQ_i} to find the largest positive imaginary part. A branch with the largest positive imaginary part of the corresponding CPSD is likely (or closest to) the source of the oscillation.
9. If the branch is a part of a ring or meshed topologies, CPSD flow has to be analyzed as described in Section II.B using network topology information.

III. CASE STUDIES

The advantages of the proposed approach are highlighted in several case studies using simulated data obtained from the 179-bus and 240-bus WECC systems. The proposed approach is compared with the state-of-the-art DEF method [3].

A. 179-bus WECC System

The 179-bus WECC system was used in [18] to create simulated cases for “A Test Cases Library for Methods Locating the Sources of Sustained Oscillations.” In all simulations the constant power load model was used, which can make loads incrementally passive [8], that is, loads cannot generate energy flow. If loads are not incrementally passive, they can generate additional flow that misleads oscillation

source identification. In this case study the load model is changed from constant power to constant impedance. Furthermore, the most challenging case from the library is when forced oscillations of the same frequency are injected into the excitation system of multiple generators (Case F_7_2). The proposed approach and the DEF method are applied to the simulated data. The result of using DEF method with the signals from the terminal buses of all 29 generators in the system is shown in Fig. 7. It is not possible to identify the source of oscillations in Fig. 7. However, the proposed approach allows correct identification of the sources. Fig. 8 shows the result of applying the proposed approach in the form of compass plots of the three CPSDs. Indeed, using S_{VP} CPSD the approach clearly identifies two sources of the forced oscillations: Generator 118 and Generator 70. The PSDs of active and reactive power shows

$$\max(|S_P|) = 1051 < \max(|S_Q|) = 1588$$

The larger maximum reactive power PSD indicates that the oscillation is coming from the excitation systems. This case study demonstrates that S_{VP} can aid in locating the source oscillation in the system where the active power consumed by loads depends on bus voltage magnitude, addressing one of the limitations of the DEF method described in [9].

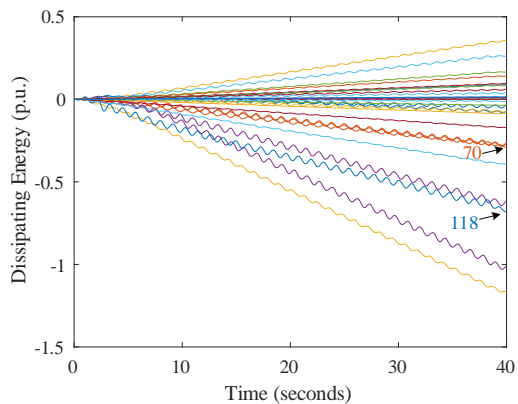


Fig. 7. Dissipating energy of all generators in the 179-bus system.

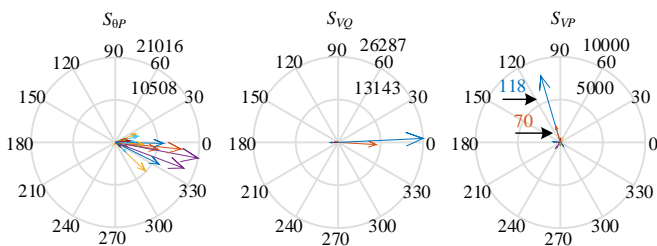


Fig. 8. Compass plots of three CPSDs for all generators in the 179-bus system.

B. 240-bus WECC System

The 240-bus WECC system [19] was used to create simulated cases for the IEEE-NASPI OSL contest [16]. To increase the complexity in identifying the source of oscillations, the generated data in the contest contained bad and missing data. Therefore, the Hampel identifier [20] is used to detect bad data while tensor decomposition [21] is applied to recover missing data.

The results of applying the proposed approach to all cases of the IEEE-NASPI OSL contest are shown in Table I. Besides Case 7 and Case 9 (the second oscillation) where S_{VP} CPSD is used to identify the source of the oscillation, $S_{\theta P}$ CPSD is selected to be used for all other cases. The proposed approach correctly identifies the bus where the asset causing the oscillation is connected to, the type of the asset and the type of the controller that caused the oscillation for all cases except Case 4. In Case 4 observability is limited and it is not possible to precisely pinpoint the bus. For this case only a region where the source is located can be identified and a set of likely buses can be provided. Case 4 demonstrates importance of good observability in a system to allow precise identification of the oscillation source.

TABLE I
RESULTS OF APPLYING CPSD APPROACH TO IEEE-NASPI OSL CONTEST

Case	Freq. (Hz)	CPSD	Bus	Asset	Controller
1	0.82	$S_{\theta P}$	1431	Gen.	Governor
2	1.19	$S_{\theta P}$	2634	Gen.	Governor
3	0.379	$S_{\theta P}$	1131	Gen.	Exciter
4	0.379	$S_{\theta P}$	3835, 3831, 3836	Gen.	Governor
5	0.68, 0.76	$S_{\theta P}$	4231	Gen.	Governor
6	1.27	$S_{\theta P}$	7031	Gen.	Governor
7	0.379	S_{VP}	2634	Gen.	Exciter
8	0.614	$S_{\theta P}$	6333	Gen.	Governor
9	0.762	$S_{\theta P}$	6533	Gen.	Governor
9	0.762	S_{VP}	4131	Gen.	Exciter
10	1.218	$S_{\theta P}$	3931	Gen.	Governor
10	0.614	$S_{\theta P}$	6335	Gen.	Governor
11	0.614	$S_{\theta P}$	4009	Load	Load
12	0.37, 0.74, 1.11, 1.48	$S_{\theta P}$	6335	Gen.	Governor
13	0.614	$S_{\theta P}$	4010	HVDC	HVDC
13	0.614	$S_{\theta P}$	2619	HVDC	HVDC

In this section we focus on the most challenging Cases 3 and 7 where the oscillations are caused by malfunction of the excitation system of a generator.

1) Case 3 of the IEEE-NASPI OSL contest

In Case 3 the oscillation is caused by the injection of a 0.379-Hz signal into the excitation system of a generator at Bus 1131. This bus is not monitored in the simulation that generated the Case 3 data. Nevertheless, the proposed approach correctly locates the source of the oscillation. First, it correctly identifies the oscillation as coming from the excitation system by comparing the PSDs of active and reactive power:

$$\max(|S_P|) = 267 < \max(|S_Q|) = 436.$$

Among the three CPSDs, $S_{\theta P}$ is the dominant CPSD that is used to locate the source of the oscillation. The path with the

largest imaginary part of S_{0P} includes parallel Branches 1401-1402. These branches are not part of a radial connection; hence, according to Step 9 of the algorithm in Section II.E, the CPSDs flows shown in Fig. 9 have to be investigated. For every bus, the cumulative outflow and inflow are calculated. In Fig. 9, the red arrows indicate calculated CPSD flow values, the green arrows indicate estimated CPSD flow values as the sum of the calculated flows, and the blue arrows indicate likely directions of unknown flows. The imaginary parts of the CPSDs are indicated in the boxes. Bus 1401 being the bus with the largest cumulative outflow is analyzed as presented in Section II.B. This bus has a load connected to it; hence, it can be considered as the source of the oscillation. If the type of oscillation was not correctly identified, this bus could be erroneously considered as the source, which would be the case for the DEF method. However, the advantage of the proposed approach is that the type of oscillation is correctly identified as coming from the excitation system. Therefore, the load at Bus 1401 cannot be the source. Hence, the source is located in the region connected to Bus 1401 by the parallel Branches 1101-1401.

To locate the source of the oscillation, flows from both sides of the region have to be analyzed. The flows in Branches 1101-1401 can be estimated by adding all the flows leaving Bus 1401. This estimation is approximate as the flows at the beginning of a branch and at the end of a branch are different due to the fact that a branch can generate or consume power, which is not accounted for in the algorithm. In addition, the flow to Load 1401 is not monitored. Similar approximation can be made at the opposite end of the region where the flow from Bus 1002 can be estimated by adding flows in Branches 1001-1202 and 1002-6505 as well as all branches with flows leaving Bus 1004. As the estimated flow from Bus 1101 is larger than the estimated flow from Bus 1002, the source is located closer to Bus 1101. Furthermore, there are two candidates for the source: Buses 1131 and 1032, as these are the only buses in the region that have generators connected to them. Bus 1131 is closer to Bus 1101 than Bus 1032, therefore, the source is identified as a generator connected to Bus 1131.

Thus, the correct identification of the oscillation type allowed accurate determination of the oscillation source in the case where it was not measured.

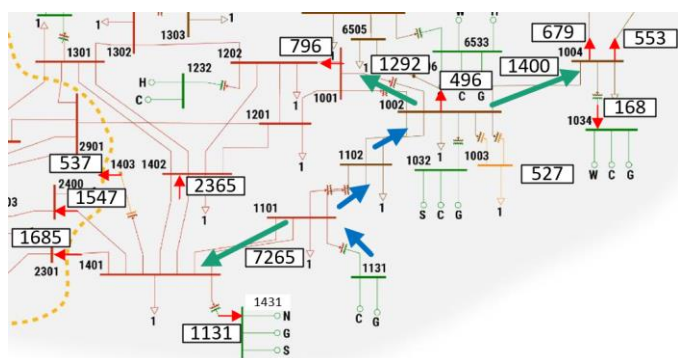


Fig. 9. CPSD flow for case 3 of the IEEE-NASPI OSL contest.

2) Case 7 of the IEEE-NASPI OSL contest:

In Case 7 the oscillation cause is an injection of a 0.379-Hz signal into the excitation system of a generator at Bus 2634. The

proposed approach correctly identifies the oscillation as coming from the excitation system by comparing the PSDs of active and reactive power:

$$\max(|S_P|) = 144 < \max(|S_Q|) = 348.$$

All three CPSDs are shown in Fig. 10 as the compass plots.

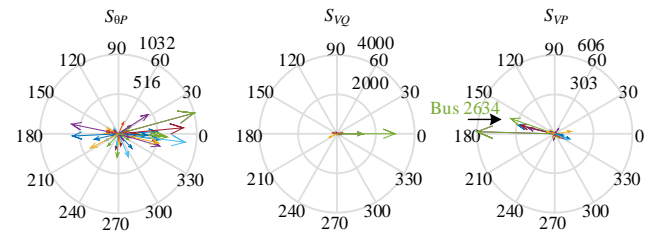


Fig. 10. Compass plots of three CPSDs for case 7 of the IEEE-NASPI OSL contest.

The S_{VP} CPSD indicates the source of the oscillation as Bus 2634. As a comparison, the result of applying the DEF method is shown in Fig. 11. One can observe that it is not possible to identify the source from Fig. 11.

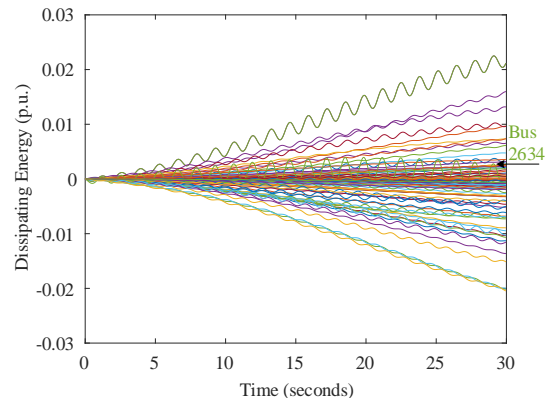


Fig. 11. Dissipating energy of all measured branches for case 7.

C. Actual Event of 0.14-Hz Oscillation

In this case study we compare the DEF method and the proposed approach using actual PMU measurements that recorded a 0.14-Hz oscillation. The PMU measurements are obtained from ISO-NE case 6 in “A Test Cases Library for Methods Locating the Sources of Sustained Oscillations” [18]. The measurements were made in the ISO New England system at a bus with four branches connected to it.

The result of applying the DEF method is shown in Fig. 12. It can be seen that the dissipating energy has non-monotonic behavior during the measured interval for all four branches, which makes it difficult to correctly identify the source. For example, on the time interval from 75 to 500 seconds the DEF method shows that the dissipating energy is going to Branch 2 (red curve in Fig. 11) while from 500 to 640 seconds the dissipating energy is coming from Branch 2 indicating that the source is located at the sending end of Branch 2.

Applying the proposed approach and analyzing S_{0P} CPSDs, the branch with the largest flow is identified as Branch 2. All obtained CPSDs are shown in the compass plots in Fig. 13. The negative imaginary part of Branch 2 (red vector in Fig. 13)

indicates that the CPSD flow is coming from Branch 2. However, the analysis of the signal in the interval from 75 to 500 seconds provides inconclusive results from $S_{\theta P}$ CPSD which has imaginary part values close to zero (see Fig. 14). There is a rotation of $S_{\theta P}$ vectors, while the position of S_{VQ} and S_{VP} vectors remains the same.

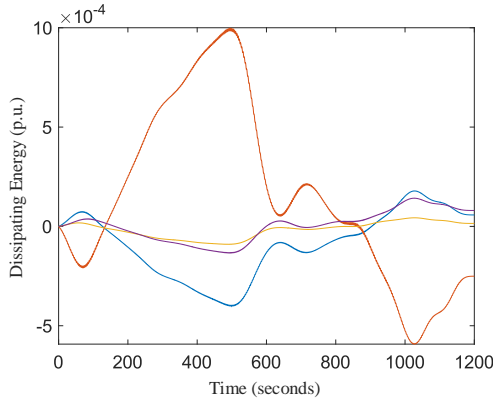


Fig. 12. Dissipating energy for all four branches.

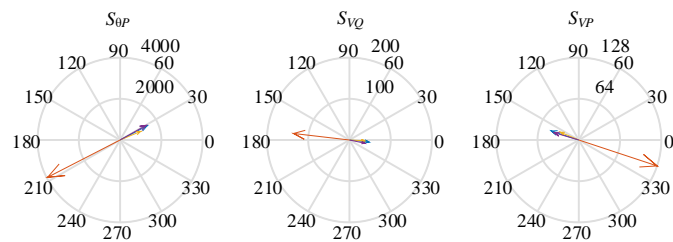


Fig. 13. Compass plots of three CPSDs for all four branches calculated for interval from 0 to 1200 s.

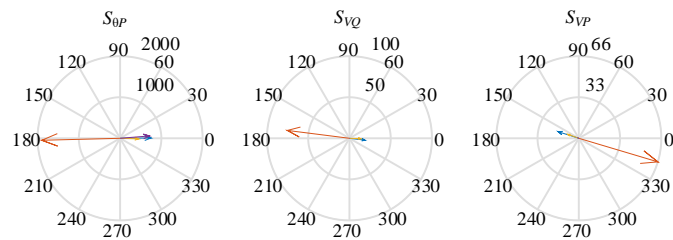


Fig. 14. Compass plots of three CPSDs for all four branches calculated for interval from 75 to 500 s: $S_{\theta P}$ rotates, S_{VQ} and S_{VP} do not rotate.

To investigate this behavior periodograms of dynamic components of active power and voltage angle are computed (see Fig. 15). In the periodogram the active power signal has a distinct peak corresponding to 0.14 Hz while the voltage angle signal does not have any peaks in the frequency band around 0.14 Hz. Thus, the oscillation is absent in the voltage angle signal. Most likely it can be explained by small amplitude of the oscillation that disappeared when instantaneous voltage measurements were processed into phasors and the voltage angle signal was estimated. For such cases dissipating energy and the phase of $S_{\theta P}$ CPSD cannot be trusted. However, the magnitude of $S_{\theta P}$ CPSD can still be used to identify the source. The frequency of this oscillation is below the frequency of the

slowest mode (0.25 Hz) in the Eastern Interconnection system (which includes the ISO New England system), so it does not create resonant with any natural mode of oscillation in the system. The source is identified by a branch with the largest magnitude of CPSD, which is Branch 2.

This example highlights importance of accurate estimation of the voltage angle and frequency signals as they play an important role in synchrophasor-based applications including identification of the oscillation source location.

In addition to the accurate estimation of the voltage angle signal, the proposed approach requires long window of data. For the reporting rate of 30 (60) measurements per second at least 10 (5) cycles of the oscillation are needed for accurate calculations. For this case of a very low-frequency oscillation, it translates to the data window of 71 seconds. Considering that the data processing takes less than a second to perform the main delay in providing the results comes from waiting to accumulate enough data to make a conclusion.

Other potential challenges that the proposed approach can encounter include:

- Intermittent behavior of a forced oscillation source when the forced oscillation appears and disappears, which is a special case of a forced oscillation of varying amplitude. For such cases, the selection of a proper window is the key for the accurate oscillation source identification.
- Forced oscillations with non-stationary frequency.
- Lower fidelity signals, when bad data is not properly marked, missing data not properly recovered, and noise not properly removed.
- Limited observability of the system, when bus with the source of oscillation is not monitored and human involvement is necessary to analyze CPSD flows. Automation of this process is an important next step for considering this approach as a control room application.

Future work will focus on addressing these challenges as well as improving the performance of the proposed approach on short-window data and the validation of the approach in real power systems.

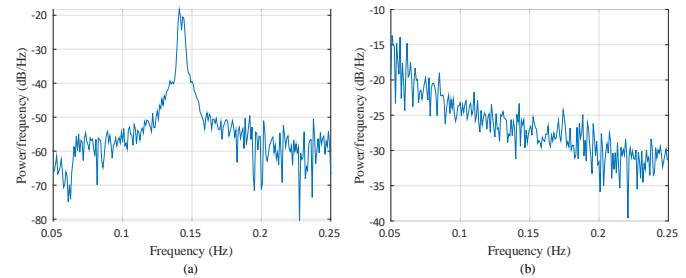


Fig. 15. Periodograms of dynamic components of active power (a) and voltage angle (b).

IV. CONCLUSIONS

The paper proposes the oscillation source location approach utilizing cross-correlation dependency of signals measured by PMUs. In the approach measured signals are preprocessed using the variational mode decomposition, from which the cross-power spectral densities of each combination of

active/reactive power and voltage magnitude/angle are computed. The computed cross-power spectral densities are then used to locate the source of the oscillation. In addition, the approach identifies the type of oscillation by comparing power spectral densities of active and reactive power. The proposed approach shows superior performance compared to the existing DEF method, specifically in the identification of the source of oscillations originating from the excitation system.

V. APPENDIX

This section provides a connection between the proposed CPSDs in (2) and the components of the dissipating energy-based methods as they use similar relationships between the same signals.

The input-output relationship described in Section II.A can be represented as an energy function

$$E = \int_{u_0}^u y(t)du(t) \quad (A1)$$

where y is the output and u is the input. Based on (A1), the energy in the increment between the trajectories of the signals and their quasi-steady state components can be defined as

$$W = \int_{\Delta u_0}^{\Delta u} \Delta y(t)d\Delta u(t) \quad (A2)$$

where $\Delta y = y - y_s$, and $\Delta u = u - u_s$. Here y_s and u_s are the output and input trajectories corresponding to the quasi-steady state, respectively.

Similar to the CPSDs in (2), the three incremental energies in the time domain can be computed as

$$\begin{aligned} W_{\theta P} &= \int_{\Delta \theta_0}^{\Delta \theta} \Delta P(t)d\Delta \theta(t), \\ W_{VQ} &= \int_{\Delta V_0}^{\Delta V} \Delta Q(t)d\Delta V(t) \\ W_{VP} &= \int_{\Delta V_0}^{\Delta V} \Delta P(t)d\Delta V(t), \end{aligned} \quad (A3)$$

The time-domain expressions in (A3) can be transformed into the frequency domain by performing Fourier transform. Applying Parseval's theorem the following result can be obtained:

$$\begin{aligned} W_{\theta P} &= \int_0^{\infty} \Delta P(t) \frac{d\Delta \theta(t)}{dt} dt = \int_0^{\infty} \Delta P(t) \Delta \dot{\theta}(t) dt = \int_{-\infty}^{\infty} \mathcal{F}\{\Delta P\} \overline{\mathcal{F}\{\Delta \dot{\theta}\}} df \\ &= \int_{-\infty}^{\infty} \mathcal{F}\{\Delta P\} j2\pi f \mathcal{F}\{\Delta \theta\} df = 2\pi \int_{-\infty}^{\infty} f \operatorname{Im}(S_{\theta P}) df \end{aligned} \quad (A4)$$

Similar transformations can be obtained for W_{VP} and W_{VQ} .

Now compare the derived expressions in (A3) to the dissipating energy defined in [3] as

$$W_D = \int \left(2\pi \Delta P(t) \Delta f(t) dt + \Delta Q(t) d(\Delta \ln V(t)) \right) \quad (A5)$$

Substituting $2\pi \Delta f = \frac{d\Delta \theta}{dt}$ into the first component of W_D , one can observe that this component is identical to $W_{\theta P}$. The second component of W_D is similar to W_{VQ} (they are identical under the assumption that the quasi-steady state component of voltage magnitude is equal to 1). W_{VP} is not represented in the dissipating energy expression. However, W_{VP} can be an important addition that is useful in locating oscillations caused by malfunction of the excitation system as demonstrated in Section III.

In the DEF method, incremental energies are used to detect the source of the oscillation. The disadvantage of the incremental energy is that for the case of oscillations with multiple frequencies, band-pass filtering might be required, which introduces additional tuning parameters associated with the band-pass filter.

VI. REFERENCES

- [1] A. G. Phadke and J. S. Thorp, *Synchronized phasor measurements and their applications*. Cham, Switzerland: Springer, 2017.
- [2] S. Maslennikov and E. Litvinov, "ISO New England experience in locating the source of oscillations online," *IEEE Trans. Power Syst.*, vol. 36, no. 1, pp. 495–503, Jan. 2020.
- [3] L. Chen, Y. Min, and W. Hu, "An energy-based method for location of power system oscillation source," *IEEE Trans. Power Syst.*, vol. 28, no. 2, pp. 828–836, May 2012.
- [4] S. Maslennikov, B. Wang, and E. Litvinov, "Dissipating energy flow method for locating the source of sustained oscillations," *Int. J. Electr. Power Energy Syst.*, vol. 88, pp. 55–62, Jun. 2017.
- [5] S. R. Sanders and G. C. Verghese, "Lyapunov-based control for switched power converters," *IEEE Trans. Power Electron.*, vol. 7, no. 1, pp. 17–24, Jan. 1992.
- [6] Y.-H. Moon, E. Lee, and T. Roh, "Development of an energy function reflecting the transfer conductances for direct stability analysis in power systems," *IET Gener.*, vol. 144, no. 5, pp. 503–509, Sep. 1997.
- [7] A. Bergen, D. Hill, and C. De Marcot, "Lyapunov function for multimachine power systems with generator flux decay and voltage dependent loads," *Int. J. Electr. Power Energy Syst.*, vol. 8, no. 1, pp. 2–10, Jan. 1986.
- [8] S. Chevalier, P. Vorobev, and K. Turitsyn, "A passivity interpretation of energy-based forced oscillation source location methods," *IEEE Trans. Power Syst.*, vol. 35, no. 5, pp. 3588–3602, Feb. 2020.
- [9] Y. Zhi and V. Venkatasubramanian, "Analysis of energy flow method for oscillation source location," *IEEE Trans. Power Syst.*, vol. 36, no. 2, pp. 1338–1349, Mar. 2020.
- [10] J. Follum and J. W. Pierre, "Initial results in the detection and estimation of forced oscillations in power systems," in *2013 IEEE North American Power Symposium (NAPS)*, Manhattan, KS, 2013, pp. 1–6.
- [11] D. J. Trudnowski, "Estimating electromechanical mode shape from synchrophasor measurements," *IEEE Trans. Power Syst.*, vol. 23, no. 3, pp. 1188–1195, Aug. 2008.
- [12] R. Xie and D. J. Trudnowski, "Tracking the damping contribution of a power system component under ambient conditions," *IEEE Trans. Power Syst.*, vol. 33, no. 1, pp. 1116–1117, Jan. 2018.
- [13] K. Dragomiretskiy and D. Zosso, "Variational mode decomposition," *IEEE Trans. Signal Process.*, vol. 62, no. 3, pp. 531–544, Nov. 2013.
- [14] N. Zhou, F. Tuffner, Z. Huang, and S. Jin, "Oscillation detection algorithm development summary report and test plan," Pacific Northwest National Laboratory, Richland, WA, Tech. Rep. PNNL-18945, Oct. 2009.
- [15] J. D. Follum, "Detection of forced oscillations in power systems with multichannel methods," Pacific Northwest National Laboratory, Richland, WA, Tech. Rep. PNNL-24681, Sep. 2015.

- [16] J. Follum, S. Maslennikov, and E. Farantatos, "IEEE/NASPI oscillation source location contest," in *NASPI Work Group Virtual Meeting*, Oct. 2021. https://www.naspi.org/sites/default/files/2021-10/D3S8_01_follum_pnnt_20211007.pdf
- [17] C. Lackner, J. Chow, F. Wilches-Bernal, and A. Darvishi, "Voltage control performance evaluation using synchrophasor data," in *53rd Hawaii International Conference on System Sciences*, 2020
- [18] S. Maslennikov, B. Wang, Q. Zhang, et al., "A test cases library for methods locating the sources of sustained oscillations," in *2016 IEEE Power and Energy Society General Meeting (PESGM)*, 2016.
- [19] H. Yuan, R. S. Biswas, J. Tan, and Y. Zhang, "Developing a reduced 240-bus WECC dynamic model for frequency response study of high renewable integration," in *2020 IEEE Transmission and Distribution Conference and Exposition (T&D)*, 2020, pp. 1–5.
- [20] H. Liu, S. Shah, and W. Jiang, "On-line outlier detection and data cleaning," *Comput. Chem. Eng.*, vol. 28, no. 9, pp. 1635–1647, Aug. 2004.
- [21] D. Osipov and J. H. Chow, "PMU missing data recovery using tensor decomposition," *IEEE Trans. Power Syst.*, vol. 35, no. 6, pp. 4554–4563, Nov. 2020.

VII. BIOGRAPHIES



Denis Osipov (S'14, M'19) received his B.Sc. and M.Sc. degrees in electrical engineering from Donetsk National Technical University, Donetsk, Ukraine in 2004 and 2005 respectively. He received his Ph.D. degree in electrical engineering from University of Tennessee, Knoxville, TN, USA in 2018. He is currently a research scientist at the Department of Electrical, Computer, and Systems Engineering in Rensselaer Polytechnic Institute, Troy, NY, USA. His

research interests include power system dynamics, control, stability and monitoring; renewable energy resources.



Stavros Konstantinopoulos (S'19, M'22) received the Diploma in Electrical and Computer Engineering from the National Technical University of Athens, Greece in 2015 and the M.Sc. and Ph.D. degrees in Electrical Engineering from the Rensselaer Polytechnic Institute, Troy, NY, USA in 2018 and 2021, respectively. He is currently an Engineer II of the Grid Operations and Planning group, Electric Power Research Institute, Palo Alto, CA, USA. His research interests include power system dynamics, control and monitoring and inverter-based resources modeling and stability.



Joe H. Chow (LF'16) received the B.Sc. degrees in electrical engineering and mathematics from the University of Minnesota, Minneapolis, MN, USA, and the M.Sc. and Ph.D. degrees in electrical engineering from the University of Illinois, Urbana-Champaign, Champaign, IL, USA. After working in the General Electric power system business in Schenectady, NY, USA, he joined Rensselaer Polytechnic Institute in 1987, and is Institute Professor of Electrical, Computer, and Systems Engineering. His research

interests include power system dynamics and control, flexible ac transmission system (FACTS) controllers, and synchronized phasor data. He is also a member of the U.S. National Academy of Engineering. He was a past recipient of the IEEE PES Charles Concordia Power Engineering Award.